The phosphatidylethanolamine-binding protein DTH1 mediates degradation of lipid droplets in *Chlamydomonas reinhardtii*

Jihyeon Lee[a], Yasuyo Yamaoka[b], Fantao Kong[c], Caroline Cagnon[d], Audrey Beyly-Adriano[d], Sunghoon Jang[b], Peng Gao[e], Byung-Ho Kang[e], Yonghua Li-Beisson[d,1], and Youngsook Lee[b,1]

[a]Division of Integrative Biosciences and Biotechnology, Pohang University of Science and Technology, 37673 Pohang, Korea; [b]Department of Life Sciences, Pohang University of Science and Technology, 37673 Pohang, Korea; [c]Laboratory of Marine Biotechnology, School of Bioengineering, Dalian University of Technology, 116024 Dalian, China; [d]Aix-Marseille University, The Commission for Atomic Energy and Alternative Energies (CEA), CNRS, Institut de Biosciences et Biotechnologies Aix-Marseille (BIAM), CEA Cadarache, Saint Paul-Lez-Durance 13108, France; and [e]State Key Laboratory of Agrobiotechnology, School of Life Sciences, The Chinese University of Hong Kong, New Territories, Hong Kong 999077, China

Edited by Krishna K. Niyogi, University of California, Berkeley, CA, and approved August 3, 2020 (received for review March 27, 2020)

Lipid droplets (LDs) are intracellular organelles found in a wide range of organisms and play important roles in stress tolerance. During nitrogen (N) starvation, *Chlamydomonas reinhardtii* stores large amounts of triacylglycerols (TAGs) inside LDs. When N is resupplied, the LDs disappear and the TAGs are degraded, presumably providing carbon and energy for regrowth. The mechanism by which cells degrade LDs is poorly understood. Here, we isolated a mutant (*dth1-1*, Delayed in TAG Hydrolysis 1) in which TAG degradation during recovery from N starvation was compromised. Consequently, the *dth1-1* mutant grew poorly compared to its parental line during N recovery. Two additional independent loss-of-function mutants (*dth1-2* and *dth1-3*) also exhibited delayed TAG remobilization. *DTH1* transcript levels increased sevenfold upon N resupply, and DTH1 protein was localized to LDs. DTH1 contains a putative lipid-binding domain (DTH1^{LBD}) with alpha helices predicted to be structurally similar to those in apolipoproteins E and A–I. Recombinant DTH1^{LBD} bound specifically to phosphatidylethanolamine (PE), a major phospholipid coating the LD surface. Overexpression of DTH1^{LBD} in *Chlamydomonas* phenocopied the *dth1* mutant's defective TAG degradation, suggesting that the function of DTH1 depends on its ability to bind PE. Together, our results demonstrate that the lipid-binding DTH1 plays an essential role in LD degradation and provide insight into the molecular mechanism of protein anchorage to LDs at the LD surface in photosynthetic cells.

Chlamydomonas reinhardtii | lipid-binding protein | TAG remobilization | lipid droplet | N resupply

Lipid droplets (LDs) are subcellular organelles ubiquitous in eukaryotic cells. LDs have a neutral lipid core consisting mainly of triacylglycerol (TAG), which is covered by a phospholipid monolayer decorated with various proteins (1, 2). In recent years, the functions of LDs have started to emerge, revealing them as key sites for preventing lipotoxicity, maintaining energy homeostasis, and providing precursors for membrane resynthesis (3–6).

LDs are generally thought to bud off from the endoplasmic reticulum (ER) membrane, then undergo expansion, shrinkage, or degradation in response to environmental as well as developmental cues (7–9). LD formation therefore requires coordination of TAG synthesis, membrane lipid synthesis, and curvature adaptation, and protein synthesis and recruitment. LD degradation involves opening up of the protein and lipid coat, followed by degradation of the core TAGs through lipolysis and/or autophagy (10, 11). LD-associated proteins are degraded through chaperone-mediated autophagy in mammalian cells (12) or the ubiquitin-proteasome system in plant cells (13, 14).

Many LD-associated proteins have been identified, thanks to the development of high-sensitivity proteomics methodologies: about 150 in mammalian cells (15), ~40 in yeast (16), ~80 in plant (17), and ~200 in the model green microalga *Chlamydomonas reinhardtii* (18–20). LD-associated proteins fall into several major functional groups: 1) major structural proteins such as oleosin, perilipin, and the major lipid droplet protein (MLDP) (2, 18, 21); 2) TAG biosynthetic enzymes, e.g., diacylglycerol acyltransferases (DGATs) (3, 22, 23) and phospholipid:diacylglycerol acyltransferase (PDAT) (24, 25); 3) proteins involved in membrane lipid coat synthesis, e.g., cytidine 5′-triphosphate (CTP):phosphocholine cytidylyltransferases (CCT1) for phosphatidylcholine (PC) synthesis (26) and betaine lipid synthase (BTA1) for synthesis of DGTS (1,2-diacylglyceryl-3-*O*-4'-(*N*,*N*,*N*-trimethyl)-homoserine) (18, 19, 27), which is important for LD growth and expansion; 4) proteins involved in protein coat degradation, e.g., the recently reported PUX10 protein (14, 28); and 5) enzymes of lipid catabolism, e.g., the mammalian adipose triacylglycerol lipase (ATGL) (29). Interestingly, the major TAG lipase in *Arabidopsis* (sugar dependent 1, SDP1) is not a constitutive component of LDs in dry seeds, but is recruited to LDs through peroxisome extensions when TAG remobilization is high (30), reflecting the dynamic nature of the LD proteome. Numerous proteins potentially involved in vesicle trafficking and

Significance

Intracellular lipid droplets (LDs) are formed under stress conditions in many organisms, including microalgae such as *Chlamydomonas reinhardtii*. When the stress is relieved, the cells degrade triacylglycerols (TAGs) stored in the LDs and resume growth. To decipher the mechanism of LD degradation, we screened for *Chlamydomonas* mutants showing defects in this process and identified one, *dth1*, that fails to produce a protein we named DTH1 (Delayed in TAG Hydrolysis 1). DTH1 is localized to LDs, binds a specific phospholipid (phosphatidylethanolamine), and contributes to the initial stage of LD degradation. The *dth1* mutant was compromised in its regrowth, suggesting that TAG remobilization is important during recovery from stress. This work thus identified a protein that is critical to LD degradation.

Author contributions: J.L., Y.L.-B., and Y.L. designed research; J.L., Y.Y., F.K., C.C., A.B.-A., S.J., P.G., and B.-H.K. performed research; J.L., Y.L.-B., and Y.L. analyzed data; and J.L., Y.L.-B., and Y.L. wrote the paper.

The authors declare no competing interest.

This article is a PNAS Direct Submission.

[1]To whom correspondence may be addressed. Email: yonghua.li@cea.fr or ylee@postech.ac.kr.

This article contains supporting information online at https://www.pnas.org/lookup/suppl/doi:10.1073/pnas.2005600117/-/DCSupplemental.

First published August 31, 2020.

transport, and proteins of so far unknown function, are also present in LDs. In summary, the functions of the majority of LD proteins remain unknown, and we still do not know how LD proteins are targeted or anchored to LDs.

C. reinhardtii has been used intensively as a model microalga to identify molecular players involved in LD turnover. *Chlamydomonas* is unicellular and can be induced to accumulate or degrade LDs simply by manipulating the level of essential nutrients, such as nitrogen (N), sulfur and phosphorus, in its medium (31–34). Some of the proteins necessary for TAG remobilization and LD turnover have been identified. They include lipases such as LIP1 (diacylglycerol lipase) and LIP4 (TAG lipase) (35, 36) and enzymes of β-oxidation such as acyl-CoA oxidase 2 and malate dehydrogenase 2 (37, 38). In addition to enzymes of lipid catabolism, CrATG8, a *Chlamydomonas* ortholog of ATG8, a critical factor of autophagy in a wide range of organisms (39), was also reported to be necessary for lipid remobilization in *Chlamydomonas* (40), suggesting a role of autophagy in the process.

In this study, we isolated and characterized a gene encoding a putative protein, which we named Delayed in Triacylglycerol

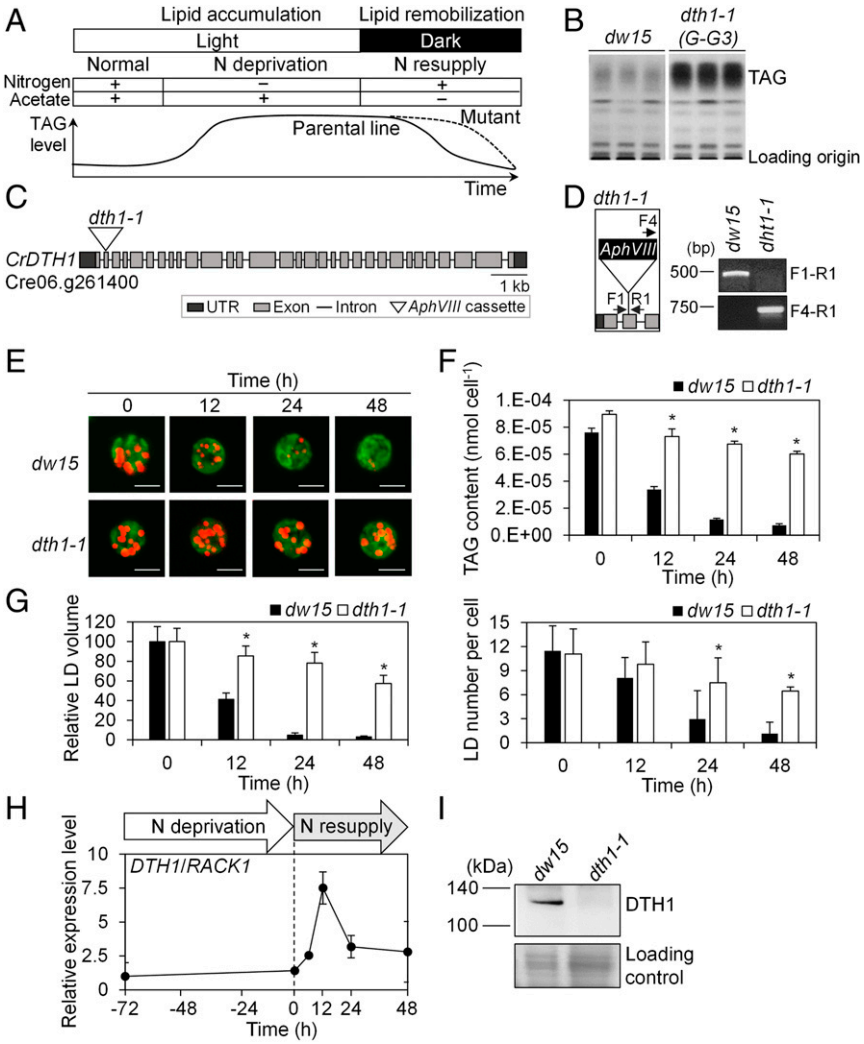

Fig. 1. Isolation of the *Chlamydomonas* mutant G-G3 (*dth1-1)* defective in TAG remobilization. (*A*) The experimental setup for mutant screening in TAG remobilization. *Chlamydomonas* cells were grown in TAP medium containing nitrogen (N) and acetate. Cells were transferred to *N*-deficient medium to induce lipid accumulation. Three days later, cells were transferred to medium containing N but no acetate. Mutants delayed in TAG degradation were isolated. (*B*) TLC plates on which lipids from three replicate samples of the mutant G-G3 (*dth1-1*) and its parental line *dw15* were separated. At 48 h after N resupply, the TAG bands in *dth1-1* sample were much stronger than those in the *dw15* sample. (*C*) The gene structure of *DTH1* in the locus Cre06.g261400. The triangle marks the insertion site of the *APHVIII* cassette in the *dth1-1* mutant. (*D*) Genotyping of *dth1-1* compared to the parental line *dw15*. Genomic DNA fragments were amplified by PCR using the primers indicated by arrows. The primers used for gene-specific amplification were F1 and R1; those for insertion-specific amplification were F4 and R1. (*E*) Time-dependent changes in LDs stained with Nile red. Images are pseudocolored orange for LDs and green for chlorophyll autofluorescence. Bars, 5 μm. (*F*) TAG amounts in *dth1-1* and its parental line *dw15*. Error bars represent SEs calculated from four biological replicates. Asterisks indicate statistically significant differences between *dth1-1* and its parental line *dw15* determined using Student's *t* test ($P < 0.005$). (*G*) Comparison of LD volume (*Left*) and number (*Right*) between *dth1-1* and its parental line *dw15* during TAG remobilization. The volume and number of LDs were quantified using ImageJ software. The volume of LDs inside *Chlamydomonas* cells ($n = \sim 35$) was measured at each time point. Error bars represent SEs. Asterisks indicate statistically significant differences between *dth1-1* and its parental line *dw15* determined using Student's *t* test ($P < 0.005$). (*H*) Induction of the *DTH1* transcript upon N resupply. The results of quantitative RT-PCR were normalized by *RACK1*. Error bars represent SEs calculated from three biological replicates. (*I*) Immunoblot analysis of DTH1 in *dth1-1* and its parental line 12 h after N resupply. The absence of a DTH1 signal in the *dth1-1* mutant indicated that it is a true knockout of *DTH1*. Immunoblot analysis was performed using an anti-DTH1a antibody. The loading control shown below is the gel stained with Coomassie brilliant blue (CBB). In *E*–*G*, $T = 0$ h indicates the start of N resupply.

Hydrolysis 1 (DTH1), that governs LD degradation in *Chlamydomonas*. The mutant *dth1* was compromised in LD degradation during N recovery. DTH1 was localized to LDs and bound specifically to phosphatidylethanolamine (PE). We present these and other data supporting the status of DTH1 as an important player in LD degradation in *Chlamydomonas*.

Results

The G-G3 *(dth1-1)* Mutant Is Defective in TAG Remobilization. To identify genes essential for TAG remobilization in *C. reinhardtii*, we isolated insertional mutants that are defective in the process, using the previously described method of finding mutant cell lines with higher TAG levels than their parental line (41). To ensure that TAG remobilization was the only source of energy, we kept the *Chlamydomonas* cells in the dark without acetate upon N resupply (Fig. 1*A*). One of the mutants, G-G3, retained a significantly higher amount of TAG than its parental line *dw15*, even 48 h after N resupply (Fig. 1 *A* and *B*).

To identify the insertion site of the *APHVIII* cassette in the G-G3 mutant, we sequenced the region flanking the cassette and used this in the Basic Local Alignment Search Tool (BLAST) search of the *C. reinhardtii* genome (Phytozome V5.5). This showed that in the mutant G-G3, the *APHVIII* gene was inserted in the second exon of the locus Cre06.g261400 (Fig. 1*C*). We confirmed the insertion site by genomic PCR, using two different combinations of primer sets (Fig. 1*D* and *SI Appendix*, Table S1). We named Cre06.g261400 DTH1 (Delayed in Triacylglycerol Hydrolysis 1) and the G-G3 mutant *dth1-1*.

To confirm that LD degradation was impaired in *dth1-1* cells, we visualized LDs by Nile red staining at 0, 12, 24, and 48 h after N resupply. LD fluorescence rapidly decreased in the parental line, *dw15*, but remained high in the *dth1-1* mutant, even 48 h after N resupply (Fig. 1*E*). Lipid quantification confirmed that TAG degradation was severely compromised in the *dth1-1* mutant compared to *dw15* after N resupply (Fig. 1*F*). We then quantified the size and number of LDs based on confocal microscopic images of *dw15* and *dth1-1* cells. The initial volume of LDs was similar in *dw15* and *dth1-1,* but after N resupply, the LDs of the parental line shrank to less than half of their original size in 12 h, whereas those of *dth1-1* remained large even 48 h after N resupply (Fig. 1 *G*, *Left*). The numbers of LDs did not differ much between the mutant and its parental line under N starvation (i.e., $T = 0$), but LDs disappeared earlier in the parental line than in the *dth1-1* mutant (Fig. 1 *G*, *Right*).

We hypothesized that if DTH1 plays an important role in TAG remobilization, its transcript level should increase in the wild type upon N resupply. Indeed, the transcript level of *DTH1* increased by sevenfold in the parental *dw15* line within 12 h of N resupply (Fig. 1*H*). To probe for the presence of DTH1 protein, we generated two polyclonal anti-DTH1 antibodies, anti-DTH1a and anti-DTH1b, using two sets of synthetic peptides as antigens (*SI Appendix*, *Materials and Methods* and Fig. S1). The anti-DTH1 antibodies were raised against five DTH1-specific synthetic peptides whose amino acid sequences are from different parts of the region between amino acid (aa) 77 and aa 1,275 of DTH1 (*SI Appendix*, Fig. S1*A*). Immunoblot analyses using the anti-DTH1a antibody showed that DTH1 was present in *dw15* at 12 h after N resupply, but it was not detectable in the *dth1-1* mutant (Fig. 1*I*).

Two Additional *dth1* Knockout Mutants Are Also Defective in TAG Remobilization. To validate whether the disruption of *DTH1* was responsible for the delay in TAG remobilization in *dth1-1*, we obtained two additional mutant alleles of *DTH1* (*dth1-2, dth1-3*), both in the CC-4533 background, from the Chlamydomonas Resource Center (Fig. 2*A*). Genomic PCR using the two combinations of primer sets confirmed the information provided by the Chlamydomonas Library Project (CLiP; www.chlamylibrary.org/) (42): the *APHVIII* cassette was integrated into the fourth exon of the *dth1-2* allele and the 13th exon of the *dth1-3* allele (Fig. 2*B* and *SI Appendix*, Table S1). The DTH1 protein was detected in the background line CC4533 using anti-DTH1a antibody 12 h after N resupply, but was not detectable in the two *dth1* mutants, indicating that they are true knockouts (Fig. 2*C*).

Upon N resupply following a period of N starvation, both *dth1-2* and *dth1-3* exhibited a delay in LD disappearance and

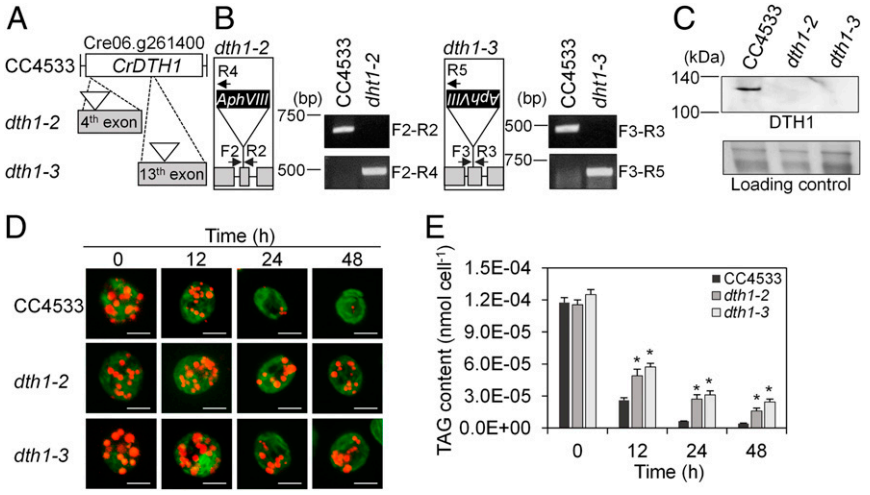

Fig. 2. Two additional *dth1* alleles also cause defects in TAG remobilization. (*A*) The insertion sites of the *APHVIII* cassette in the Cre06.g261400 (*DTH1*) locus in the two mutant alleles. Triangles denote the insertion positions of the *APHVIII* cassette in the fourth and 13th exons of *DTH1* in *dth1-2* and *dth1-3*, respectively, based on information from the CLiP library. (*B*) Genotyping of the *dth1-2* and *dth1-3* mutants compared to their parental line CC4533. Genomic DNA fragments were amplified by PCR using the primers indicated by arrows. Gene-specific amplification was performed using the primer pairs F2-R2 and F3-R3; insertion-specific amplification was performed using the primer pairs F2-R4 (for *dth1-2*) and F3-R5 (for *dth1-3*). (*C*) Immunoblot analysis of DTH1 in *dth1-2, dth1-3,* and the parental line 12 h after N resupply. The absence of a DTH1 signal in samples from the two mutants indicated that they are true knockouts of *DTH1*. An anti-DTH1a antibody was used for the immunoblots. CBB was used as a loading control. (*D*) Observation of LDs stained by Nile red after N resupply. LDs gradually disappeared in the parental line whereas these two mutants were retained. Images are pseudocolored orange for LDs and green for chlorophyll autofluorescence. Bars, 5 μm. (*E*) Quantification of TAG amounts in *dth1-2, dth1-3*, and their parental line CC4533. Error bars represent SEs calculated from four biological replicates. Statistical analysis was carried out using Student's *t* test (*$P < 0.01$). In *D* and *E*, $T = 0$ h indicates the start of N resupply.

TAG degradation compared to their parental line CC4533 (Fig. 2 *D* and *E*). Taken together, these data established that DTH1 plays an essential role in LD degradation and TAG remobilization in *Chlamydomonas*.

***Chlamydomonas* DTH1 Is a Protein Present in Some Species Belonging to the Orders Chlamydomonadales and Sphaeropleales within the Class Chlorophyceae.** *Chlamydomonas* DTH1 (CrDTH1) is predicted to contain 2,407 aa and has an estimated molecular weight of 243.7 kDa. We were not able to clone the entire gene, nor were able to synthesize it, because it is very long and rich in GC content (65.76%). On immunoblots probed with the two anti-DTH1 antibody preparations, strong signals were consistently detected at around 130 kDa (Figs. 1*I* and 2*C* and *SI Appendix*, Fig. S1*B*). Preblocking the anti-DTH1a antibody with the peptides used to raise them abolished the signal at 130 kDa (*SI Appendix*, Fig. S1*C*), supporting our conclusion that the 130-kDa protein band was indeed DTH1.

However, the entire predicted complementary DNA (cDNA) sequence seems to be transcribed, since the full sequence of *CrDTH1* appears in the collection of expressed sequence tags detected from RNA sequencing of samples from various N deficiency time-course experiments (www.ncbi.nlm.nih.gov/geo/query/acc.cgi?acc=GSE34585) (43) and data collected in Phytozome through JBrowse view. The discrepancy between the apparent size of DTH1 determined by immunoblot and the estimated molecular weight is not understood currently.

We next searched for recognizable motifs in DTH1 using Multiple Em for Motif Elicitation (MEME) analysis, and identified three motifs (*SI Appendix*, Fig. S2) (meme-suite.org/) (44). The first motif, which is at the N terminus and consists of 5 repeats of 7 aa (*SI Appendix*, Fig. S2*A*), has no reported function. The second motif consists of 5 repeats of 10 aa (*SI Appendix*, Fig. S2*B*), and its function also has not yet been studied. The third motif consists of 5 repeats of 29 aa, located at aa 1,057 to 1,304 (*SI Appendix*, Fig. S2*C*). This motif is composed of the alpha-helical structure similar to protein segment in apolipoproteins A-I and E, which bind and cover lipoproteins in mammalian cells (45–48). Because of this similarity, we designated the middle portion containing the third motif as a lipid-binding domain (LBD) and focused our subsequent research on this domain. Wheel representations of these repeats inside LBD predicted alpha helices with alternating hydrophilic and hydrophobic portions, indicating that they are amphipathic (*SI Appendix*, Fig. S2*D*) (49, 50).

Proteins with amino acid sequences homologous to that of CrDTH1 were found in only five species belonging to two orders of Chlorophyta: *Volvox carteri*, *Gonium pectorale*, *Tetrabaena socialis*, and *Chlamydomonas eustigma*, belonging to the order Chlamydomonadales, and *Monoraphidium neglectum*, belonging to Sphaeropleales (*SI Appendix*, Fig. S3). The putative LBD seems to be conserved in three of these five CrDTH1 homologs (*SI Appendix*, Fig. S3*A*). We made an extensive effort to reconstruct the evolutionary history of DTH1 and its homologs but were unsuccessful because of the absence of similar proteins outside the two orders in Chlorophyta (*SI Appendix*, Fig. S3*B*). Nevertheless, structural conservation, rather than primary amino acid sequence, appears to be the rule among LD-associated proteins.

Loss of DTH1 Does Not Affect the TCA Cycle or β-Oxidation of FAs. The next question we addressed was at which step of TAG remobilization DTH1 functions. TAG remobilization from LD involves three major temporally and spatially separated steps. First, LDs are degraded to expose internal TAGs to lipases that release fatty acids from them. Next, the fatty acids are activated to acyl-coenzyme A species (acyl-CoAs) that undergo β-oxidation to produce acetyl-CoA, which, finally, enters the tricarboxylic acid (TCA) cycle for energy production (Fig. 3*A*). To pinpoint the step at which DTH1 functions, we first tested whether the *dth1* mutant has a normal TCA cycle. For this purpose, we compared the growth of the parental line and *dth1-1* during N resupply, with or without acetate in the medium. *Chlamydomonas* can produce acetyl-CoA from exogenously supplied acetate (51). The mutant *dth1-1* showed severely retarded growth compared to its parental line when the cells were resupplied with N without acetate (Fig. 3*B*). With acetate in the medium, however, the *dth1-1* mutant grew at the same rate as its parental line (Fig. 3*B*). These results indicated that the mutant was able to use the TCA cycle to generate energy from acetyl-CoA, but could not make acetyl-CoA from lipids.

We next asked whether the delay in TAG degradation in the *dth1-1* knockout was due to a defect in the β-oxidation of fatty acids (FAs). For this purpose, we tested whether the retarded growth of *dth1-1* during the TAG remobilization phase could be rescued by exogenously supplied oleic acid. *Chlamydomonas* cells were induced to accumulate TAGs by imposing N starvation for 3 d, then transferred into acetate-free Tris-phosphate medium (TP) medium supplemented with 0.5 mM oleic acid in the dark. The *dth1-1* mutant grew much better in the presence of oleic acid than its absence (Fig. 3*C*), and its growth rate reached that of its parental line. These results indicated that *dth1-1* can use oleic acid for growth, and thus is normal in regard to FA utilization through β-oxidation. In addition, the growth of the three *dth1* mutants did not differ from that of their parental lines during optimal growth (*SI Appendix*, Fig. S4). Together, these results confirmed that the downstream metabolic pathways in the *dth1-1* mutant are normal and therefore suggested that DTH1 is involved in earlier steps of TAG remobilization (i.e., upstream of β-oxidation of FAs).

DTH1 Is Localized to LDs during N Recovery. To provide further hints on the specific step where DTH1 functions, we localized the protein by subcellular fractionation and immunogold labeling. First, we isolated LDs from cells during N recovery (Fig. 4*A*) and performed immunoblot analysis to detect DTH1 (Fig. 4*B*). In the LD fractions of both parental lines, we detected strong DTH1 bands using the anti-DTH1a antibody, but only very weak bands when we probed the fractions with antibodies to markers of various subcellular organelles: NAB1 (nucleic acid binding protein 1; cytosol), BiP1 (binding immunoglobulin protein 1; ER), and RbcL (rubisco large subunit; chloroplast) (Fig. 4*B*). In contrast, in the fraction remaining after LD isolation (residual fraction), the DTH1 signal was very weak and the other protein signals were strong (Fig. 4*B*). These results suggested that DTH1 was associated with LDs. Silver staining of all proteins associated with either the LD or residual fractions also supported this conclusion: strong bands of ∼26 kDa, the size of the LD marker protein MLDP (the major LD-associated protein) (20), were detected only in the LD fraction, not in the residual fraction (Fig. 4*C*).

To confirm the subcellular localization of DTH1, we performed immunogold labeling experiments. DTH1a-specific immunogold particles were associated with LDs in *dw15* parental line cells (Fig. 5 *A*–*C*). Other organelles exhibited negligible levels of labeling when compared with LDs (Fig. 5*D*). No gold particles were discerned in *dth1-1* mutant cell sections (Fig. 5*E*) or in *dw15* cells if the experiment was carried out after omitting the anti-DTH1 antibody from the primary antibody solution (*SI Appendix*, Fig. S5). Taken together, both subcellular fractionation and immunogold labeling data indicated that DTH1 is an LD-localized protein.

DTH1 Contains a Domain that Specifically Binds Phosphatidylethanolamine (PE). Next, we attempted to resolve how DTH1 associates with LDs. Since the LBD (aa 1057–1304) of DTH1 is structurally similar to apolipoproteins A-I and E, which bind to lipoproteins in mammalian cells (Fig. 6*A*), we tested the lipid-binding ability of the $DTH1^{LBD}$. For this purpose, we made a construct consisting of maltose-binding protein (MBP) fused to the N terminus of the LBD of DTH1,

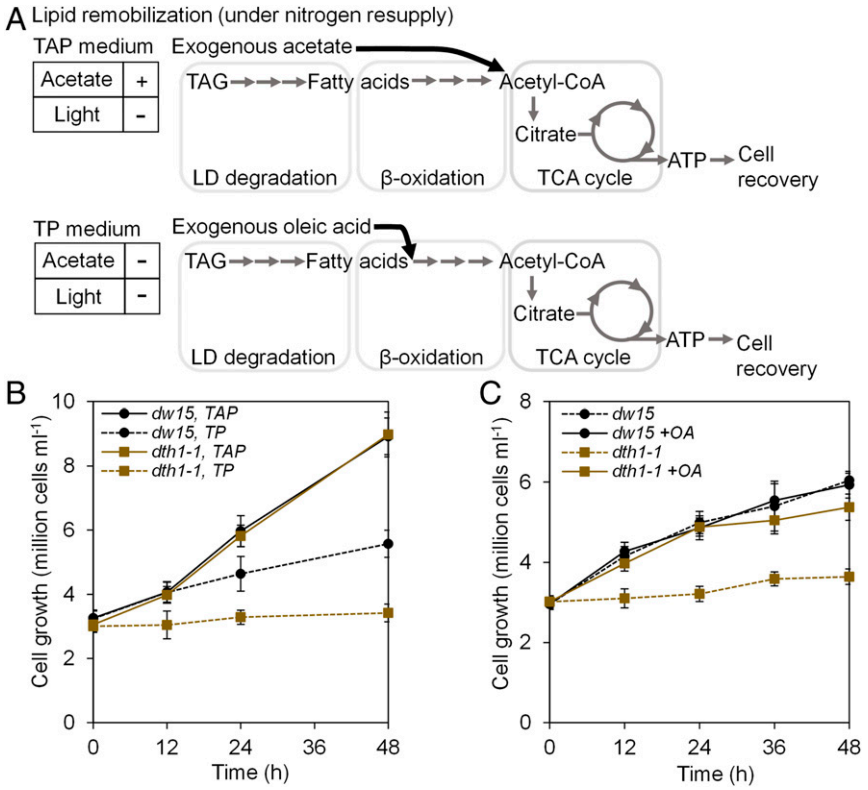

Fig. 3. Growth of *dth1-1* during recovery from nitrogen starvation in the dark, with or without acetate or oleic acid supplementation. (*A*) Schematic representation of the major steps of TAG remobilization—LD degradation, β-oxidation, and the TCA cycle—which together provide energy for growth recovery. (*B*) Comparison of the growth of *dw15* and *dth1-1* in the absence or presence of acetate during N resupply. (*C*) Comparison of the growth of *dw15* and *dth1-1* in the absence or presence of oleic acid (OA; 0.5 mM) in the TP medium during N resupply. In *B* and *C*, error bars indicate SEs ($n = 4$). Statistical analyses were carried out using Student's *t* test. The growth rates of the *dth1-1* mutant and its parental line differed significantly at 12, 24, 36, and 48 h in TP medium ($P < 0.005$), but were similar in medium supplemented with acetate or oleic acid.

expressed it in *Escherichia coli* and purified the fusion protein using amylose resin. Purified MBP-DTH1^{LBD} protein was detectable upon Coomassie blue staining and immunoblot analysis using the anti-DTH1b antibody (Fig. 6*B*). To test lipid-binding activity, we used an in vitro lipid protein overlay assay (*SI Appendix*, *Materials and Methods*) in which native glycerolipids purified from *Chlamydomonas dw15* were spotted on polyvinylidene fluoride (PVDF) membrane and incubated with purified MBP-DTH1^{LBD}. MBP-DTH1^{LBD} bound

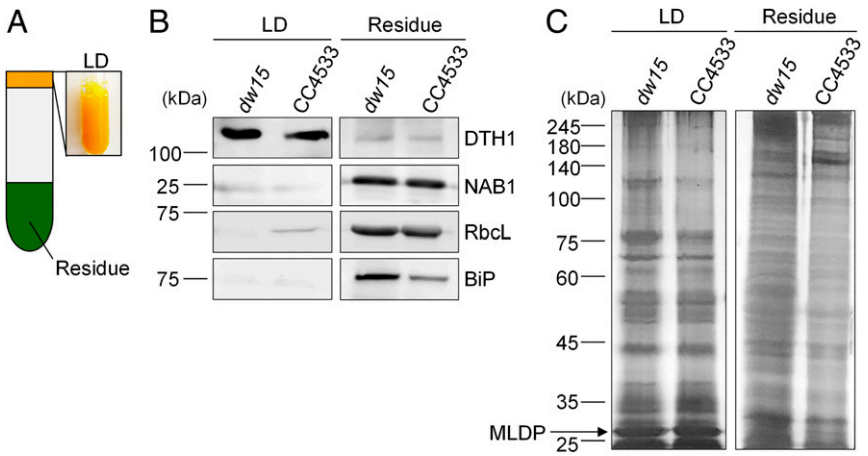

Fig. 4. DTH1 is localized to lipid droplets. (*A*) LDs obtained by sucrose density gradient centrifugation. The cell lysate remaining after LD isolation (the residue fraction) was used for comparison with the LD fraction. *Chlamydomonas* cells were sampled 6 h after N resupply following 3 d of N deprivation. (*B*) Immunoblot analysis of proteins associated with the LD and residue fractions prepared from the parental lines *dw15* and CC4533. Equal amounts of protein were loaded in each lane. NAB1 was used as a cytosolic marker, RbcL as the chloroplast marker and binding BiP as an ER marker. (*C*) Protein gels silverstained to show the major proteins in the LD and residue fractions. Equal amounts of proteins were loaded in each lane. The black arrow indicates the putative position of MLDP, the major LD-associated protein of *Chlamydomonas*.

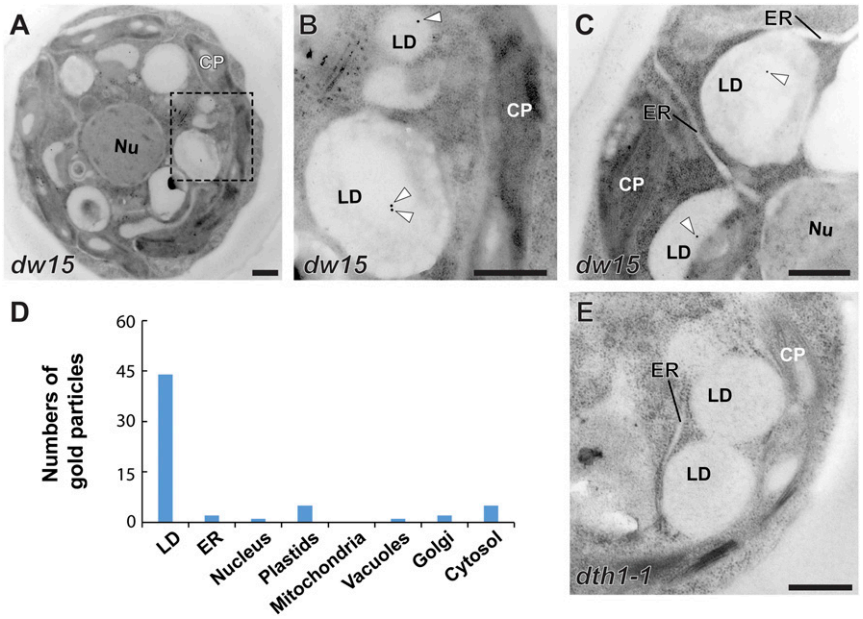

Fig. 5. Transmission electron microscopy of immunogold-labeled DTH1 in *Chlamydomonas* confirms its localization in lipid droplets. (*A*–*C*) Immunogold labeling of DTH1 in a wild-type *Chlamydomonas* cell (*dw15*) grown for 6 h under N resupply conditions following 3 d of N starvation. Gold particles (15 nm, white triangles) are associated with lipid droplets. (*B*) is a higher-magnification image of the boxed area in *A*. (*C*) shows lipid droplets connected to ER elements in another cell. (*D*) Distribution of immunogold particles in *Chlamydomonas* cell sections prepared in the same way as those in *A*–*C*. Sixty gold particles from 10 different cells were counted. Approximately 75% of gold particles were seen in lipid droplets. (*E*) Absence of DTH1 immunogold signals in *dth1-1*. The mutant sample was grown under the same condition as the *dw15* line shown in *A*–*C*. No gold particles were seen in the mutant cell samples. (Scale bars, 500 nm.) CP, chloroplast; Nu, nucleus.

specifically to PE, but not to any other major lipids of *Chlamydomonas* (Fig. 6*C*). Free MBP did not bind to any lipids we tested under our experimental conditions (*SI Appendix*, Fig. S6). These results demonstrated that DTH1 contains a PE-specific binding domain and is an LD-associated lipid-binding protein.

Overexpression of DTH1^{LBD} in *Chlamydomonas* Inhibits TAG Remobilization. We then asked whether the binding of DTH1^{LBD} to PE is necessary for TAG remobilization in *Chlamydomonas*. We reasoned that overexpressed DTH1^{LBD} might compete with native DTH1 for binding to PE in vivo. If binding to the LBD of the native protein was crucial for TAG remobilization, then excess DTH1^{LBD} might have a dominant-negative effect. To test this possibility, we introduced *DTH1^{LBD}* into the UVM4 strain of *Chlamydomonas* and obtained two overexpression lines (Fig. 7*A*). Both overexpressing lines were compromised in LD degradation compared to the background UVM4 upon N resupply (Fig. 7*B*). At 24 h following N resupply, TAG levels remained high in the *DTH1^{LBD}* overexpression lines relative to the level in UVM4 (Fig. 7*C*). By contrast, in normal Tris-acetate-phosphate (TAP) medium, there was no apparent difference in growth or other phenotypes among the three lines of cells (*SI Appendix*, Fig. S7), indicating that the overexpressed LBD peptide does not interfere with normal lipid metabolism under the control condition. Together, these results indicated that binding of DTH1 to PE is important for LD degradation in *Chlamydomonas*.

Discussion

DTH1 Is Essential for LD Turnover and TAG Remobilization. We have presented multiple lines of experimental evidence that DTH1 has an essential role in LD degradation. First, three independent *dth1* knockout mutants showed drastically delayed TAG degradation after N resupply (Figs. 1 and 2). Second, overexpression of the PE-binding domain of DTH1 phenocopied the *dth1* knockout mutation, compromising TAG degradation (Figs. 6 and 7). Finally, DTH1 expression is induced upon N resupply following N deprivation (Fig. 1*H*), and DTH1 is localized in LDs (Figs. 4 and 5). Our lipid-binding assay suggested that DTH1 binds PE (Fig. 6). Furthermore, the effects of overexpression of

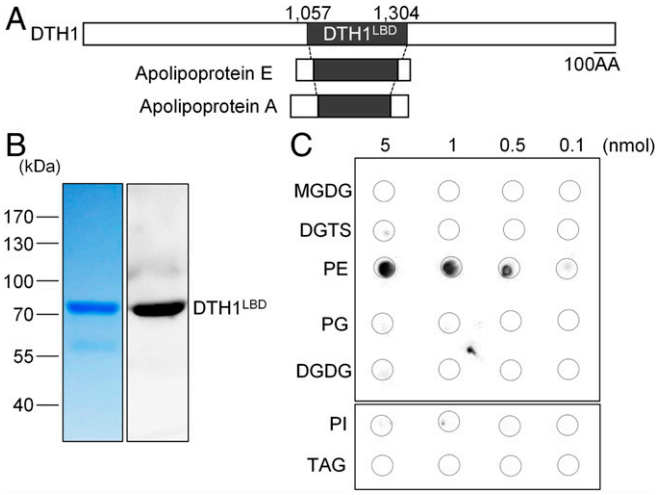

Fig. 6. In vitro lipid overlay assay of recombinant DTH1^{LBD} protein shows that it binds phosphatidylethanolamine. (*A*) Schematic representation of the location of the DTH1 LBD (DTH1^{LBD}) by Swiss three-dimensional (3D) modeling software. (*B*) Coomassie-stained sodium dodecyl sulfate polyacrylamide gel electrophoresis (SDS/PAGE) (*Left*) and immunoblot (*Right*) probed with anti-DTH1b antibody. Recombinant DTH1^{LBD} protein fused to MBP was purified by affinity chromatography using amylose resin. (*C*) Lipid overlay assay using recombinant DTH1^{LBD} protein fragments and PVDF-immobilized lipids strips (5, 1, 0.5, 0.1 nmol). DTH1 binding was detected by immunoblotting with anti-DTH1b antibody. Abbreviations: MGDG, monogalactosyldiacylglycerol; PG, phosphatidylglycerol; DGDG, digalactosyldiacylglycerol; PI, phosphatidylinositol.

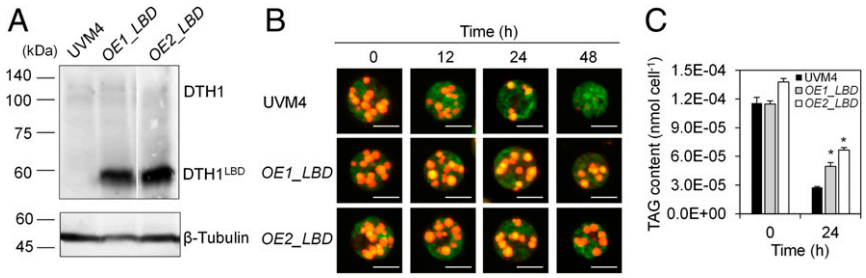

Fig. 7. In vivo overexpression of DTH1^{LBD} in *Chlamydomonas* compromises LD degradation. (*A*) Immunoblot analysis of whole proteins extracted from the cells of *DTH1^{LBD}* overexpressing UVM4 lines (*OE1_LBD, OE2_LBD*) and the background UVM4 line grown for 12 h under N resupply conditions. DTH1^{LBD} was detected with anti-DTH1b antibody. β-tubulin was used as the loading control. (*B*) Time-dependent observation of LDs stained with Nile red. LDs of two *DTH1^{LBD}* overexpressing lines were retained, whereas those of the UVM4 background line were gradually reduced. $T = 0$ h indicates the start of N resupply. Images are pseudocolored orange for LDs and green for chlorophyll autofluorescence. Bars, 5 μm. (*C*) Quantification of TAG amounts in *DTH1^{LBD}* overexpressing lines compared to that in the UVM4 background. Cells were sampled at 0 and 24 h after N resupply. Error bars represent SEs calculated from three biological replicates. Statistical analysis of the difference between the overexpression lines and the background line was carried out using Student's *t* test (*$P < 0.005$).

the LBD of DTH1 (Fig. 7) suggest that this domain is important for lipid degradation in vivo. The function of the LBD may be to anchor DTH1 to LDs during the LD degradation phase.

Homologs of CrDTH1 exist only in two orders of Chlorophyta (*SI Appendix*, Fig. S3). Some CrDTH1 homologs might perform functions similar to CrDTH1 during recovery from N starvation, since three out of the five of them also contain all or part of the LBD. Our extensive evolutionary analysis of the DTH1 LBD did not yield any convincing matches outside the Chlorophyta, suggesting that DTH1 is unique to this phylum. Another protein unique to Chlorophyta is MLDP (18). We speculate that CrDTH1 and MLDP might have evolved very quickly, undergoing extensive modifications that make it difficult to reconstruct their evolutionary history. However, structural similarities might still exist among LD-associated proteins. Future determination of the structure of DTH1 might help identify other proteins with similar functions in other phyla.

PE Is Probably Essential for Anchoring DTH1 to LDs in *Chlamydomonas*. Unlike other phospholipids, PE is cone shaped and forms a negative curvature (52). Because of its unique structure, PE plays important roles in membrane fusion, disassembly of the contractile ring, and maintenance of contact sites between subcellular organelles (53). For example, severe reduction of PE abundance causes the loss of contacts between the ER and mitochondria *in Saccharomyces cerevisiae* (54). In yeast and mammalian cells, PE is the second most prevalent phospholipid in LD coats, comprising up to 30% of the total phospholipid in the coat (55, 56). In the LDs of *Drosophila* S2 cells, PE (50 to 60%) is the most prevalent phospholipid on the surface (57). PE has also been identified in purified LDs from *Chlamydomonas* (19, 20). Until now, the role of PE in LD dynamics was not known. There have been reports hinting that PE is involved in LD degradation: the autophagy protein ATG8 is activated only when it is conjugated with PE and is actively involved in LD degradation in many organisms, including *Chlamydomonas* (40). Our results strongly support an important role for PE in LD degradation in *Chlamydomonas*. We showed that a PE-binding protein, DTH1, is localized to LDs (Figs. 4 and 5) and that the PE-binding domain is critical for TAG remobilization (Fig. 6). We speculate that PE provides a binding site for DTH1 and that this binding is an important step in the LD degradation process. However, PE binding alone is not sufficient to explain the specific localization of DTH1 to LDs since other cellular membranes also contain PE. Amphipathic helices are a signature secondary structure in many Class II LD-located proteins for selective targeting to LDs (58). Similar amphipathic helical structures are repeated in the LBD of DTH1 (*SI Appendix*, Fig. S2*D*). Thus, it is possible that the amphipathic helix in DTH1 helps target it to LDs, and PE binding in particular might be critical for anchoring DTH1 to LDs. Interactions with proteins coating LDs may also be necessary for its specific localization to LDs.

TAG Remobilization Is Important for Growth Recovery under N Resupply. In medium with no acetate or other carbon source, the growth of the *dth1-1* mutant was severely retarded compared to that of its parental line (Fig. 3). The growth difference seemed to correlate with the difference in their ability to degrade LDs: in the parental cell line, the LDs disappeared rapidly, whereas this

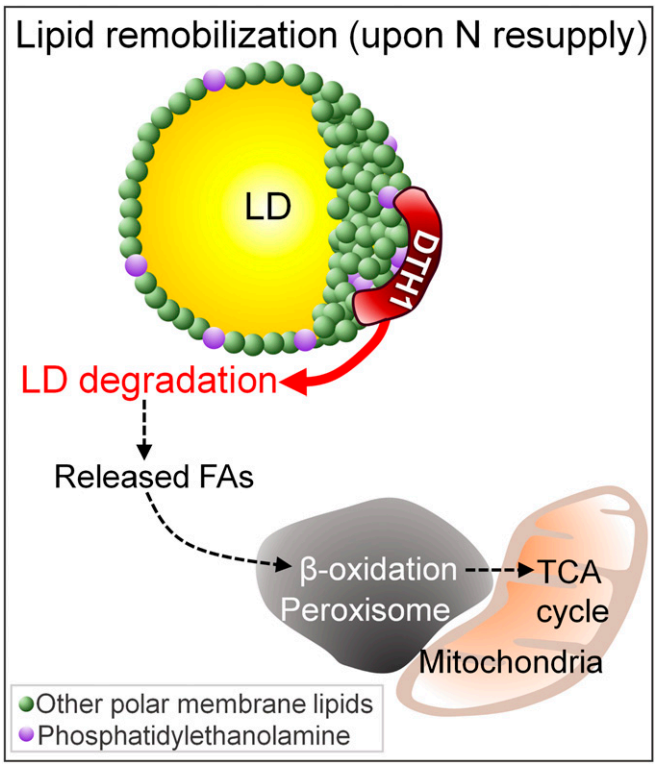

Fig. 8. Working model of DTH1 function during LD turnover and TAG remobilization in *Chlamydomonas*. DTH1 is likely to be anchored to LDs through PE binding and functions to degrade LD, possibly by interacting with other proteins. DTH1 is not involved in the further downstream metabolism of lipids, such as β-oxidation of fatty acids or TCA cycle operation.

process was much delayed in the knockout (Fig. 1). Furthermore, when the growth medium was supplemented with acetate, an energy source, the growth of *dth1-1* recovered to the rate of its parental line (Fig. 3*B*). These results suggest that LD degradation and the energy released from this process are important for growth recovery in *Chlamydomonas* when N is resupplied after N starvation.

A Model for DTH1 Function in LD Turnover and TAG Remobilization. We started this research aiming to identify a factor important for TAG remobilization in *Chlamydomonas*. Our results suggest that DTH1 functions during the initiation of TAG remobilization in *Chlamydomonas* (Fig. 8), but not in downstream metabolic pathways in the peroxisomes or mitochondria. The fact that the *dth1-1* knockout line did not show any growth retardation compared to the parental line in the presence of acetate demonstrated that DTH1 is not involved in the TCA cycle (Fig. 3*B*). We also excluded the possibility that DTH1 is involved in β-oxidation of fatty acids by showing that the growth defect of *dth1-1* could be rescued by oleic acid supplementation (Fig. 3*C*). These results support the possibility that DTH1 functions during or before degradation of TAG to fatty acids.

DTH1 could be involved in one or more of the initial steps of LD degradation including protein coat removal, lipid coat degradation, TAG lipolysis, and lipophagy. We speculate that DTH1, anchored to LDs through PE binding, might recruit interacting partners that contribute to LD degradation. The interacting proteins could include lipases and the proteins involved in lipophagy. In *Chlamydomonas*, lipases such as LIP1 (diacylglycerol lipase) and LIP4 (TAG lipase) are involved in TAG degradation (35, 36), but none of these are associated with LDs. The *Chlamydomonas atg8* knockout shows delayed TAG degradation (40), indicating that lipophagy mediated by ATG8 might be important for TAG remobilization. In *Arabidopsis*, oleosin, a structural protein of LDs, is degraded by ubiquitin-mediated proteolysis during TAG remobilization (13, 14). By analogy, degradation of MLDP, the *Chlamydomonas* LD structural protein, might be required for structural disintegration of LDs prior to LD degradation. Thus it is plausible that proteins involved in ubiquitination and subsequent degradation of the LD structure might be recruited to the LD surface to initiate degradation. Further studies are needed to determine whether any such proteins are recruited by DTH1 to LDs during TAG remobilization.

To conclude, our work identified a protein that is essential for lipid degradation during recovery from N starvation in *Chlamydomonas*. This provides a perspective for understanding the mechanism of lipid degradation, which is likely to be important not only in microalgae but also in many other organisms.

Materials and Methods

Strains and Culture Conditions. *C. reinhardtii* strain *dw15* (*nit1-305 cw-15; mt$^+$*) was used to generate an insertional mutant library from which the G-G3 *(dth1-1)* mutant was isolated (41). Two other alleles, *dth1-2* (LMJ.RY0402.135887) and *dth1-3* (LMJ.RY0402.198754), and their parental line CC4533 (*cw15; mt$^-$*) were obtained from the Chlamydomonas Resource Center (42). The parental strains were maintained on agar plates containing TAP (59), and additional supplementation of paromomycin (10 μg mL^{-1}) was included for mutants. For liquid culture, cells were incubated at 23 °C under continuous light (60 μmol photons m^{-2} sec^{-1}) in a shaking incubator at 190 rpm. To induce lipid accumulation, cells were transferred to *N*-free TAP medium. To initiate TAG remobilization, cells were transferred to acetate-free *N*-containing TP medium and kept in the dark.

Other methods are described in *SI Appendix, Materials and Methods*.

Data Availability. All data supporting the findings of this study are contained in the main text and *SI Appendix*. All study data are included in the article and *SI Appendix*.

ACKNOWLEDGMENTS. We thank the Chlamydomonas Resource Center at the University of Minnesota for providing the indexed *C. reinhardtii* insertional mutants. We also thank Mr. Chung Hyun Cho and Professor Hwan Su Yoon for phylogenetic analysis of DTH1 and its homologs. This work was supported by a grant of the BioGreen 21 Program funded by the Rural Development Administration (No. PJ013412) and Basic Science Research Program (NRF-2018R1A2A1A05018173) through the National Research Foundation of Korea, funded by the Ministry of Science and ICT (Information and Communication Technology) awarded to Y.L.; by Hong Kong Research Grant Council (GRF14121019, AoE/M-05/12, C4002-17G) and Cooperative Research Program for Agriculture Science & Technology Development (Project No. 0109532019) Rural Development Administration funds awarded to B.-H.K.; by the National Natural Science Foundation of China (31900221) and Fundamental Research Funds for the Central Universities (DUT18RC(3) 041) awarded to F.K.; and by ANR Diesalg and SignauxBioNRJ funds awarded to Y.L.-B.

1. D. L. Brasaemle, N. E. Wolins, Packaging of fat: An evolving model of lipid droplet assembly and expansion. *J. Biol. Chem.* **287**, 2273–2279 (2012).
2. D. J. Murphy, Structure, function and biogenesis of storage lipid bodies and oleosins in plants. *Prog. Lipid Res.* **32**, 247–280 (1993).
3. C. Chitraju *et al.*, Triglyceride synthesis by DGAT1 protects adipocytes from lipid-induced ER stress during lipolysis. *Cell Metab.* **26**, 407–418.e3 (2017).
4. L. L. Listenberger *et al.*, Triglyceride accumulation protects against fatty acid-induced lipotoxicity. *Proc. Natl. Acad. Sci. U.S.A.* **100**, 3077–3082 (2003).
5. D. F. Markgraf *et al.*, An ER protein functionally couples neutral lipid metabolism on lipid droplets to membrane lipid synthesis in the ER. *Cell Rep.* **6**, 44–55 (2014).
6. J. Petschnigg *et al.*, Good fat, essential cellular requirements for triacylglycerol synthesis to maintain membrane homeostasis in yeast. *J. Biol. Chem.* **284**, 30981–30993 (2009).
7. Q. Gao, J. M. Goodman, The lipid droplet-a well-connected organelle. *Front. Cell Dev. Biol.* **3**, 49 (2015).
8. J. A. Olzmann, P. Carvalho, Dynamics and functions of lipid droplets. *Nat. Rev. Mol. Cell Biol.* **20**, 137–155 (2019).
9. M. Schuldiner, M. Bohnert, A different kind of love–Lipid droplet contact sites. *Biochim. Biophys. Acta Mol. Cell Biol. Lipids* **1862**, 1188–1196 (2017).
10. C.-W. Wang, Lipid droplets, lipophagy, and beyond. *Biochim. Biophys. Acta* **1861**, 793–805 (2016).
11. R. Zechner *et al.*, FAT SIGNALS–Lipases and lipolysis in lipid metabolism and signaling. *Cell Metab.* **15**, 279–291 (2012).
12. S. Kaushik, A. M. Cuervo, Degradation of lipid droplet-associated proteins by chaperone-mediated autophagy facilitates lipolysis. *Nat. Cell Biol.* **17**, 759–770 (2015).
13. C. Deruyffelaere *et al.*, Ubiquitin-mediated proteasomal degradation of oleosins is involved in oil body mobilization during post-germinative seedling growth in *Arabidopsis*. *Plant Cell Physiol.* **56**, 1374–1387 (2015).
14. C. Deruyffelaere *et al.*, PUX10 is a CDC48A adaptor protein that regulates the extraction of ubiquitinated oleosins from seed lipid droplets in *Arabidopsis*. *Plant Cell* **30**, 2116–2136 (2018).
15. K. Bersuker *et al.*, A proximity labeling strategy provides insights into the composition and dynamics of lipid droplet proteomes. *Dev. Cell* **44**, 97–112.e7 (2018).
16. E. Currie *et al.*, High confidence proteomic analysis of yeast LDs identifies additional droplet proteins and reveals connections to dolichol synthesis and sterol acetylation. *J. Lipid Res.* **55**, 1465–1477 (2014).
17. H. Liu, C. Wang, F. Chen, S. Shen, Proteomic analysis of oil bodies in mature Jatropha curcas seeds with different lipid content. *J. Proteomics* **113**, 403–414 (2015).
18. E. R. Moellering, C. Benning, RNA interference silencing of a major lipid droplet protein affects lipid droplet size in *Chlamydomonas reinhardtii*. *Eukaryot. Cell* **9**, 97–106 (2010).
19. H. M. Nguyen *et al.*, Proteomic profiling of oil bodies isolated from the unicellular green microalga *Chlamydomonas reinhardtii*: With focus on proteins involved in lipid metabolism. *Proteomics* **11**, 4266–4273 (2011).
20. C. H. Tsai *et al.*, Dynamics of protein and polar lipid recruitment during lipid droplet assembly in *Chlamydomonas reinhardtii*. *Plant J.* **83**, 650–660 (2015).
21. E. J. Blanchette-Mackie *et al.*, Perilipin is located on the surface layer of intracellular lipid droplets in adipocytes. *J. Lipid Res.* **36**, 1211–1226 (1995).
22. C. A. Harris *et al.*, DGAT enzymes are required for triacylglycerol synthesis and lipid droplets in adipocytes. *J. Lipid Res.* **52**, 657–667 (2011).
23. M. La Russa *et al.*, Functional analysis of three type-2 DGAT homologue genes for triacylglycerol production in the green microalga *Chlamydomonas reinhardtii*. *J. Biotechnol.* **162**, 13–20 (2012).
24. A. Dahlqvist *et al.*, Phospholipid:diacylglycerol acyltransferase: An enzyme that catalyzes the acyl-CoA-independent formation of triacylglycerol in yeast and plants. *Proc. Natl. Acad. Sci. U.S.A.* **97**, 6487–6492 (2000).
25. K. Yoon, D. Han, Y. Li, M. Sommerfeld, Q. Hu, Phospholipid:diacylglycerol acyltransferase is a multifunctional enzyme involved in membrane lipid turnover and degradation while synthesizing triacylglycerol in the unicellular green microalga *Chlamydomonas reinhardtii*. *Plant Cell* **24**, 3708–3724 (2012).
26. N. Krahmer *et al.*, Phosphatidylcholine synthesis for lipid droplet expansion is mediated by localized activation of CTP:phosphocholine cytidylyltransferase. *Cell Metab.* **14**, 504–515 (2011).
27. W. R. Riekhof, B. B. Sears, C. Benning, Annotation of genes involved in glycerolipid biosynthesis in *Chlamydomonas reinhardtii*: Discovery of the betaine lipid synthase BTA1Cr. *Eukaryot. Cell* **4**, 242–252 (2005).

28. F. K. Kretzschmar *et al*., PUX10 is a lipid droplet-localized scaffold protein that interacts with CELL DIVISION CYCLE48 and is involved in the degradation of lipid droplet proteins. *Plant Cell* **30**, 2137–2160 (2018).
29. R. Zimmermann *et al*., Fat mobilization in adipose tissue is promoted by adipose triglyceride lipase. *Science* **306**, 1383–1386 (2004).
30. P. J. Eastmond, SUGAR-DEPENDENT1 encodes a patatin domain triacylglycerol lipase that initiates storage oil breakdown in germinating *Arabidopsis* seeds. *Plant Cell* **18**, 665–675 (2006).
31. X. Deng, X. Fei, Y. Li, The effects of nutritional restriction on neutral lipid accumulation in *Chlamydomonas* and *Chlorella*. *Afr. J. Microbiol. Res.* **5**, 260–270 (2011).
32. M. Siaut *et al*., Oil accumulation in the model green alga *Chlamydomonas reinhardtii*: Characterization, variability between common laboratory strains and relationship with starch reserves. *BMC Biotechnol.* **11**, 7 (2011).
33. L. Valledor, T. Furuhashi, L. Recuenco-Muñoz, S. Wienkoop, W. Weckwerth, System-level network analysis of nitrogen starvation and recovery in *Chlamydomonas reinhardtii* reveals potential new targets for increased lipid accumulation. *Biotechnol. Biofuels* **7**, 171 (2014).
34. P. M. Weers, R. D. Gulati, Growth and reproduction of Daphnia galeata in response to changes in fatty acids, phosphorus, and nitrogen in *Chlamydomonas reinhardtii*. *Limnol. Oceanogr.* **42**, 1584–1589 (1997).
35. X. Li, C. Benning, M.-H. Kuo, Rapid triacylglycerol turnover in *Chlamydomonas reinhardtii* requires a lipase with broad substrate specificity. *Eukaryot. Cell* **11**, 1451–1462 (2012).
36. J. Warakanont, Y. Li-Beisson, C. Benning, LIP4 is involved in triacylglycerol degradation in *Chlamydomonas reinhardtii*. *Plant Cell Physiol.* **60**, 1250–1259 (2019).
37. F. Kong *et al*., Interorganelle communication: Peroxisomal MALATE DEHYDROGENASE2 connects lipid catabolism to photosynthesis through redox coupling in *Chlamydomonas*. *Plant Cell* **30**, 1824–1847 (2018).
38. F. Kong *et al*., *Chlamydomonas* carries out fatty acid β-oxidation in ancestral peroxisomes using a bona fide acyl-CoA oxidase. *Plant J.* **90**, 358–371 (2017).
39. T. Shpilka, H. Weidberg, S. Pietrokovski, Z. Elazar, Atg8: An autophagy-related ubiquitin-like protein family. *Genome Biol.* **12**, 226 (2011).
40. M. Kajikawa *et al*., Isolation and characterization of *Chlamydomonas* autophagy-related mutants in nutrient-deficient conditions. *Plant Cell Physiol.* **60**, 126–138 (2019).
41. C. Cagnon *et al*., Development of a forward genetic screen to isolate oil mutants in the green microalga *Chlamydomonas reinhardtii*. *Biotechnol. Biofuels* **6**, 178 (2013).
42. X. Li *et al*., An indexed, mapped mutant library enables reverse genetics studies of biological processes in *Chlamydomonas reinhardtii*. *Plant Cell* **28**, 367–387 (2016).
43. N. R. Boyle *et al*., Three acyltransferases and nitrogen-responsive regulator are implicated in nitrogen starvation-induced triacylglycerol accumulation in *Chlamydomonas*. *J. Biol. Chem.* **287**, 15811–15825 (2012).
44. T. L. Bailey *et al*., MEME SUITE: Tools for motif discovery and searching. *Nucleic Acids Res.* **37**, W202–W208 (2009).
45. K. Gulshan *et al*., PI (4, 5) P2 is translocated by ABCA1 to the cell surface where it mediates apolipoprotein A1 binding and nascent HDL assembly. *Circ. Res.* **119**, 827–838 (2016).
46. Y.-H. Hsieh, C.-Y. Chou, Structural and functional characterization of human apolipoprotein E 72-166 peptides in both aqueous and lipid environments. *J. Biomed. Sci.* **18**, 4 (2011).
47. J. T. Sparrow *et al*., Apolipoprotein E: Phospholipid binding studies with synthetic peptides from the carboxyl terminus. *Biochemistry* **31**, 1065–1068 (1992).
48. A. Waterhouse *et al*., SWISS-MODEL: Homology modelling of protein structures and complexes. *Nucleic Acids Res.* **46**, W296–W303 (2018).
49. R. Gautier, D. Douguet, B. Antonny, G. Drin, HELIQUEST: A web server to screen sequences with specific α-helical properties. *Bioinformatics* **24**, 2101–2102 (2008).
50. G. Vieyres, T. Pietschmann, HCV pit stop at the lipid droplet: Refuel lipids and put on a lipoprotein coat before exit. *Cells* **8**, 233 (2019).
51. X. Johnson, J. Alric, Central carbon metabolism and electron transport in *Chlamydomonas reinhardtii*: Metabolic constraints for carbon partitioning between oil and starch. *Eukaryot. Cell* **12**, 776–793 (2013).
52. S. Mukherjee, F. R. Maxfield, Membrane domains. *Annu. Rev. Cell Dev. Biol.* **20**, 839–866 (2004).
53. K. Emoto *et al*., Redistribution of phosphatidylethanolamine at the cleavage furrow of dividing cells during cytokinesis. *Proc. Natl. Acad. Sci. U.S.A.* **93**, 12867–12872 (1996).
54. S. Lahiri *et al*., A conserved endoplasmic reticulum membrane protein complex (EMC) facilitates phospholipid transfer from the ER to mitochondria. *PLoS Biol.* **12**, e1001969 (2014).
55. A. Penno, G. Hackenbroich, C. Thiele, Phospholipids and lipid droplets. *Biochim. Biophys. Acta* **1831**, 589–594 (2013).
56. K. Tauchi-Sato, S. Ozeki, T. Houjou, R. Taguchi, T. Fujimoto, The surface of lipid droplets is a phospholipid monolayer with a unique Fatty Acid composition. *J. Biol. Chem.* **277**, 44507–44512 (2002).
57. H. E. Jones, J. L. Harwood, I. D. Bowen, G. Griffiths, Lipid composition of subcellular membranes from larvae and prepupae of *Drosophila melanogaster*. *Lipids* **27**, 984–987 (1992).
58. R. Dhiman, S. Caesar, A. R. Thiam, B. Schrul, Mechanisms of protein targeting to lipid droplets: A unified cell biological and biophysical perspective. *Semin. Cell Dev. Biol.*, 10.1016/j.semcdb.2020.03.004 (2020).
59. E. H. Harris, *The Chlamydomonas Sourcebook: Introduction to Chlamydomonas and its Laboratory Use*, (Academic press, San Diego, 2009).